# Relation between METEOSAT Water Vapor Radiance Fields and Large Scale Tropical Circulation Features

LAURENCE PICON AND MICHEL DESBOIS

*LMD/CNRS, Ecole Polytechnique, Palaiseau, France*

(Manuscript received 18 March 1989, in final form 21 February 1990)

ABSTRACT

Mean monthly images from the water vapor channel of METEOSAT characteristically contain large-scale spatial structures, especially in tropical regions. The aim of this paper is to establish connections between these structures and large-scale circulation features. For this purpose, statistical relationships between radiances and some meteorological parameters provided by ECMWF analyses are studied.

Temporal correlations are computed for two sizes of regions, in order to compare temporal changes associated with both large-scale circulations and smaller scale systems. The correlations obtained are poor, suggesting that the chosen parameters are not well related at short time scales.

Temporal averages appear more suitable for these comparisons. As expected, the mean relative humidity yields the best correlation with the mean water vapor radiances. A (weaker) relationship exists also with mean dynamic fields: large water vapor radiances are almost always related to subsidence in the middle troposphere, divergence near the surface, and convergence in the upper troposphere. However, there is regional variability in the results; one explanation may be different contributions from horizontal advection and vertical motions to the humidity of the middle troposphere.

## 1. Introduction

Meteorological satellites have existed sufficiently long to allow climatic-scale studies. From their archive, the International Satellite Cloud Climatology Program (Schiffer and Rossow 1983) has constructed appropriate datasets for this purpose. Using METEOSAT ISCCP data, Desbois et al. (1988) showed that statistics on longwave radiances can be used to identify interannual variations of climatic parameters in the African and tropical Atlantic area. In the present paper, time series of water vapor (WV) METEOSAT radiance fields are examined.

The images built from the monthly averages of WV radiances (Fig. 1) show smooth large-scale structures, which exhibit interannual variations, especially in their positions (Desbois et al. 1988). These positions appear to be associated qualitatively with major climatic features (ITCZ for the low radiance values, subtropical highs for the large ones) which have a great influence on the African climate.

The variability of the African climate is mostly characterized by precipitation variations between different rainy seasons, but the causes of these variations are not understood. In these regions, the study of the large-scale circulation from conventional data is difficult because of the scarcity of upper-air data, and because fundamental tropical circulation parameters, such as divergence and vertical velocity, cannot be measured directly or deduced reliably. The surface network is denser, but measurements from it are often perturbed by local effects.

Satellite data provide more continuous and regular information, but physical parameters other than direct radiances generally cannot be derived without the help of information from different sources. For example, Krishnamurti and Low-Nam (1986) computed patterns of potential vorticity and inferred the Hadley circulation from a regression between monthly TIROS-N or Nimbus outgoing longwave radiation and FGGE III-b data. The 1982–83 ENSO event was also studied by this method, using divergent fluxes and vertical velocity deduced from ERBE (Earth Radiation Budget Experiment) radiances (Ardanuy and Krishnamurti 1987).

In the present study, statistical relationships between radiances and chosen meteorological parameters are investigated. Because of the scarcity of upper-air data in the African–Atlantic area, these parameters are derived from analyses of the European Centre for Medium Range Weather Forecasts (ECMWF), which merges all available data through a sophisticated assimilation system. Keeping in mind that these analyses are not perfect, we nevertheless consider them as the best approximation presently available for describing large-scale atmospheric physical parameters and a nec-

*Corresponding author address:* Dr. L. Picon, Laboratoire de Meteorologie Dynamique du C.N.R.S., Ecole Polytechnique, Rte Departemente 36, F-91128 Palaiseau Cedex, France.

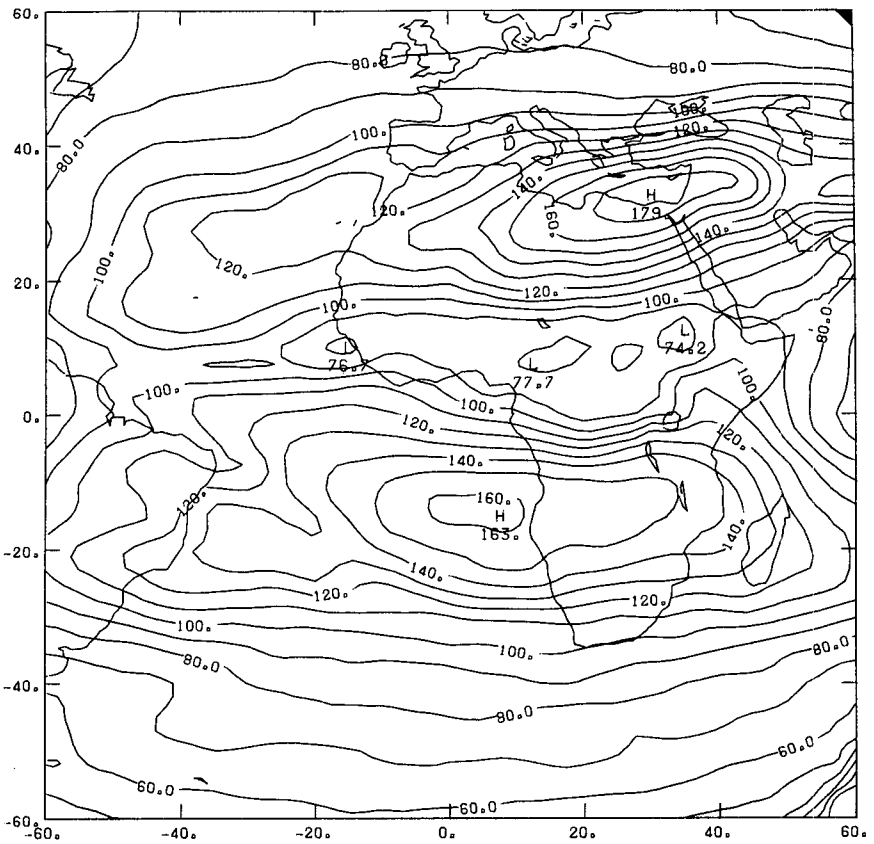


FIG. 1. Mean METEOSAT WV radiance for July 1985. Contour interval is 10 counts. Low values indicate relative moistness; high values, relative dryness.

essary tool for investigating the relationship of the WV radiance fields to the large-scale circulation.

The first part of this paper reviews previous interpretations of the WV radiances. Then, the ECMWF analysis method is presented briefly. Analysis and discussion of the correlations between monthly radiances and selected mean meteorological parameters follows. Temporal correlations are also discussed briefly. Conclusions are presented on the usefulness of WV radiance fields for describing tropical circulations and their variations.

## 2. The water vapor channel and its interpretation

Since the launch of METEOSAT 1 in November 1977, satellites of the METEOSAT series have possessed two operational longwave imaging radiometers. The so-called thermal IR (infrared) window channel is centered on the atmospheric transmission maximum around 11.5 $\mu$m, whereas the WV channel is centered on a water vapor absorption maximum around 6.3 $\mu$m. Similar channels were used on Nimbus satellites and are also present on the VAS of GOES satellites and NOAA operational polar orbiters.

The radiation emitted by the surface at this wavelength is entirely absorbed by water vapor present in the low layers of the atmosphere. Thus, the images received at the satellite do not show any surface features and represent essentially the horizontal distribution of the radiation emitted by water vapor in the middle and upper layers of the troposphere.

Structures appear in these images, even in cloud-free areas, at synoptic and planetary scales. Because METEOSAT is a geostationary satellite producing WV images at least once per hour, information on the large-scale motions of synoptic scale systems can be extracted from the animation of time series of these images (Desbois et al. 1986).

A truly quantitative interpretation of WV radiances is not easy, however. The altitude of phenomena observed by the WV radiometers is particularly difficult to evaluate. For Tiros IV, Raschke and Bandeen (1967) estimate it to be between 600 and 100 hPa; for Nimbus IV, Steranka et al. (1973) estimate 500 to 350 hPa. For METEOSAT, Poc et al. (1981) show that the peak of the contribution function is located between 300 and 550 hPa. They also show that the effect of temperature variations on the WV radiances is weak compared to the effect of humidity variations. This finding,

combined with the spectral width of the METEOSAT WV channel (5.7–7.1 $\mu$m), allows them to find a relationship between the METEOSAT radiances and the precipitable water content (or relative humidity) of a relatively thick layer (600–300 hPa).

Schmetz and Turpeinen (1988) deduce the upper tropospheric humidity (UTH) for the same 600–300 hPa layer from METEOSAT WV data. They also compute and stratify regionally IR and WV pseudo-radiances for different humidity conditions and satellite zenith angles, using a radiative transfer model and ECMWF analyzed temperature profiles. A table allows values of UTH to be assigned to radiometric counts observed by METEOSAT. A comparison between UTH and humidities observed from the radiosonde network indicates good linear correlation, especially in tropical areas (Turpeinen and Schmetz 1989).

Dynamic studies were also performed using WV radiances, assuming that, without phase change (in cloud-free regions), the amount of water vapor in a volume of air depends only on transport processes; water vapor can then be used as an atmospheric tracer.

Before the implementation of such a channel on geosynchronous satellites, the water vapor channel of Nimbus 4 was used for such studies in the 1970s. Martin and Salomonson (1970) studied 60 situations involving the subtropical jet stream over North America. They relate the maximum speed of the jet to the structure of the blackbody temperature fields for different channels, including the WV. The spatial analyses of the radiance fields show a tilt of the isotherms characterizing a baroclinic atmosphere, in agreement with jet-stream dynamics. Steranka (1973) uses only the 6.3 $\mu$m channel of the THIR of Nimbus 4 to improve humidity fields and streamlines of wind at 400 hPa deduced from radiosondes. Rodgers et al. (1976) perform a case study over the Rocky Mountains with images from the same satellite. Comparing radiances, radiosonde data, and dynamic model results, they investigate mechanisms of drying in the middle troposphere: an increase of blackbody temperature is associated with a drying that is produced mainly by horizontal advection of dry air and then maintained by subsidence.

Ramond et al. (1981) studied the dynamics of the polar jet stream with the WV channel of METEOSAT. Using a simplification of the radiative transfer equation, they show that the apparent blackbody temperature in the 6.3 $\mu$m channel is close to the temperature of the weighting function peak. In addition, if the zenith angle is small, the field of blackbody temperatures matches the temperature of an isohumidity surface. These results are confirmed by radiosonde measurements, except near frontal zones. A similar interpretation is given by Stout et al. (1984), who show a clear relationship between the apparent WV channel temperature T* and the pressure corresponding to the top millimeter of precipitable water within the atmosphere. These authors suggest that temporal variations of T* can be related to vertical velocity.

These physical interpretations relate WV radiances to atmospheric vertical and horizontal motions: let a pixel A be located in the center of a quasi-permanent high radiance area like the ones appearing on the mean WV images. At this point, the blackbody temperature is maximum, which means that the weighting function peak is located below all the ones in the surrounding area. At a given height above the local weighting function peak, the air is driest at A. On the scale of the mean circulations, the presence of this dry air cannot be attributed to horizontal advection, because all the surrounding regions are wetter. The dry air has to come from upper levels, associated with large-scale subsidence, like that associated with the Hadley or Walker cells. Horizontal transport of humidity by mean or turbulent motions in the middle troposphere tends to reduce the efficiency of this drying process, producing finally an equilibrium state that shows up in the mean fields.

## 3. Satellite data and ECMWF analyses

The satellite data used in this paper are level B METEOSAT ISCCP data. The spatial resolution is 30 km at the subsatellite point (sampling of one 5 km $\times$ 5 km resolution pixel in each 6 $\times$ 6 pixels square), and the temporal resolution is three hours. The composite image of Fig. 1 has been computed by averaging the individual pixel values on the 240 images available between 1 and 30 July 1985. Three images are missing and have been replaced by the ones of 31 July at the same hour.

The ECMWF data assimilation system (Hollingsworth 1985; Lorenc 1977; Lorenc 1981) blends forecasted parameters with observed values. A global three-dimensional multivariate statistical interpolation scheme is used every six hours. The basic approach is to express the departure between an analyzed value and its predicted first guess by a linear combination of the departures between the predicted value and surrounding observed values. This interpolation procedure is applied directly to the mass and wind fields at the forecast model levels (16 levels in July 1985) and in latitude–longitude boxes of 660 km sides. The July 1985 analysis of the humidity field is simpler: it is applied at only five standard levels below 300 hPa. Analyses are then interpolated to standard pressure levels.

The analyzed fields are subjected finally to a normal-mode initialization procedure to eliminate gravity waves prior to numerical integration. The quality of the analysis is strongly dependent on the forecast model. Important modifications were made in the analysis-forecast system during 1984–85—revisions in the analysis scheme, modification of the physical parameterizations, and increases in the spatial resolution. The impact of these modifications has been evaluated,

particularly in tropical regions (Tiedtke et al. 1988; Illari 1985; Brankovic 1986).

Specific studies of the quality of the model analysis/forecast have been performed over a number of tropical regions: over the Pacific Ocean, McGuirk et al. (1989) find that ECMWF analyses provide "surprisingly realistic moisture patterns." Over Africa, Reed et al. (1988) evaluate the performance of the analysis/forecast system to study tropical easterly waves. In data-rich regions, the analysis results are similar to those obtained directly from wind observations, and tracking of the easterly waves can be performed from 850 hPa vorticity maxima. However, some regions of small-scale convergence are not reproduced by the analyses, due to a no-divergence constraint imposed on the corrections to the first-guess wind field. Due partly to this constraint and partly to general problems of data assimilation in the tropics, it has been shown recently (Lambert 1989; Hollingworth et al. 1989) that the quality of the divergent wind fields is still dubious in the tropics.

In the present paper, METEOSAT radiances are compared with the 1200 UTC initialized analyses for July 1985 contained in the ECMWF archives. In 1985, conventional and satellite data were used in the analysis: the conventional data include surface data in reasonable quantity over Africa but scarce at upper levels; the satellite data include only temperature retrievals from TOVS and cloud winds. There is no input from the WV channel of METEOSAT, thus excluding redundant information in the comparisons. The ECMWF analyses and METEOSAT radiances have been averaged over the same period of July 1985.

## 4. Spatial correlation studies

As previously shown, the mean WV images yield consistent and smooth spatial structures. We interpret these structures by comparing them to those existing in the mean analyzed meteorological fields.

### *a. Comparisons with thermodynamic fields*

Previous studies described in section 2 have shown that the phenomena observed in the WV channel of METEOSAT are located in a thick layer of the middle troposphere, except in cloudy areas. Therefore, we compare temperature and relative humidity patterns at 500 hPa.

The 500 hPa temperature field (Fig. 2) is rather flat over a wide latitude range (from 20°N to 10°S) cen-

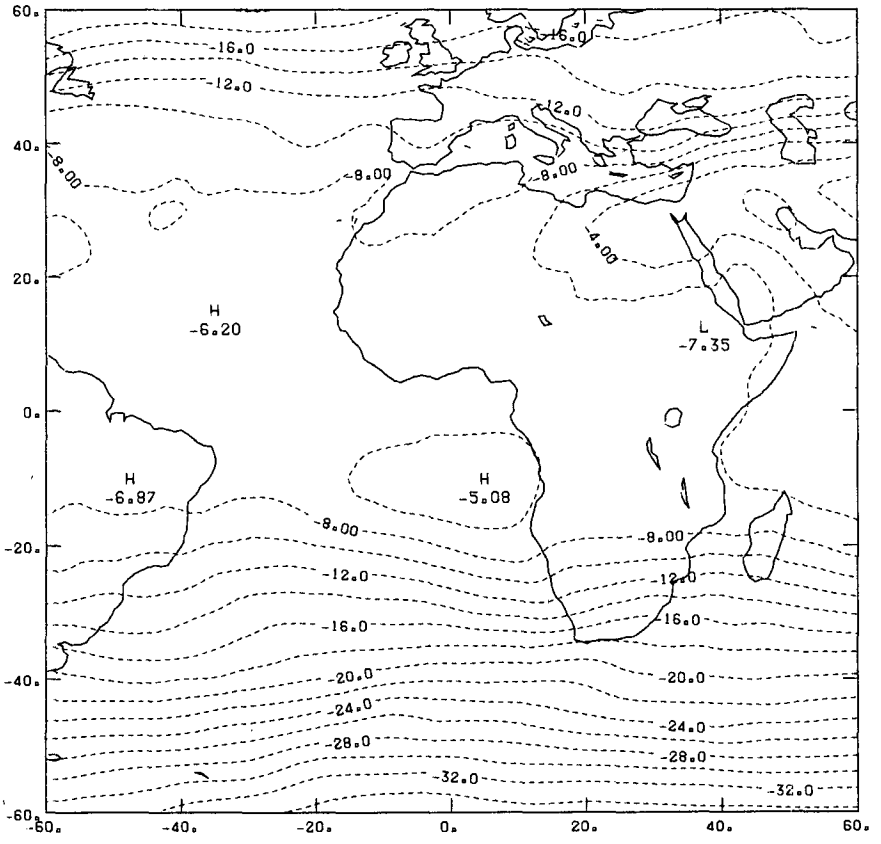


FIG. 2. Mean ECMWF analyzed temperature at 500 hPa for July 1985. Contour interval is 2°C.

tered on the ITCZ. A temperature maximum corresponding to a WV radiance maximum (indicating dryness as well) is found along the Angola coast. A cooler region corresponds to a decrease of WV radiance (moistness or cloudiness) along the Morocco coast. The high temperature area over Arabia and the Red Sea is comparable to the radiance maximum over the eastern Mediterranean Sea. However, there is poor correspondence in the shape, location, and alignment of the two features.

Figure 3 shows the mean analyzed relative humidity pattern at 500 hPa. The spatial structure is similar to the radiance patterns. Over the eastern Mediterranean, a strong radiance maximum corresponds to a humidity minimum. Along the Canary Islands, a weaker radiance maximum is associated with a second humidity minimum. Between these two regions, weaker radiances and larger humidities indicate the occurrence of occasional tropical plumes over western Sahara. In the Southern Hemisphere, a large area of high radiances related to low relative humidity stretches along 20°S over the Atlantic Ocean and the African continent. This area is divided into two parts by weaker radiances, identified from image film loops as due to sporadic, high clouds, associated with NW–SE convergence at low levels, and originating as tropical plumes from the northeastern coast of South America.

*b. Dynamic fields*

The mean July 1985 wind vectors for 1000 hPa and 200 hPa are presented in Figs. 4 and 5.

At the lowest level, the flow over the tropical Atlantic Ocean is characterized by strong trade winds in both hemispheres, centered at 20°N and 10°S. A characteristic Indian-monsoon flow exists over the Indian Ocean. In the Northern Hemisphere, a noticeable anticyclonic flow appears also over the eastern Mediterranean, producing intense northeasterlies (the Harmattan) over the eastern Sahara, and northwesterlies over the Red Sea. This flow is strongly diffluent. Over western Africa, confluence of the northerly flow and the weak African-monsoon flow occurs between 10°N and 20°N. Over eastern Africa, the mean flow is weak everywhere.

At 200 hPa, the tropical easterly jet (TEJ) dominates the equatorial region. This flow is especially intense over the Indian Ocean and weakens progressively over Africa and the Atlantic. However, a weak secondary maximum exists to the southwest of the west African coast.

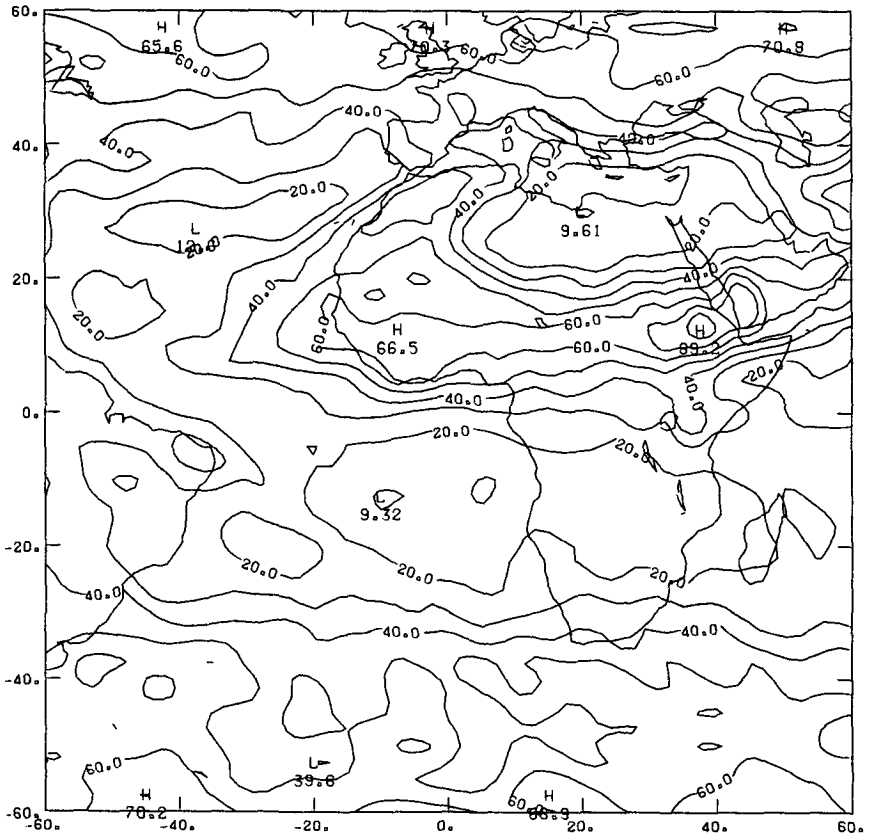


FIG. 3. Mean ECMWF analyzed relative humidity at 500 hPa for July 1985. Contour interval is 10%.

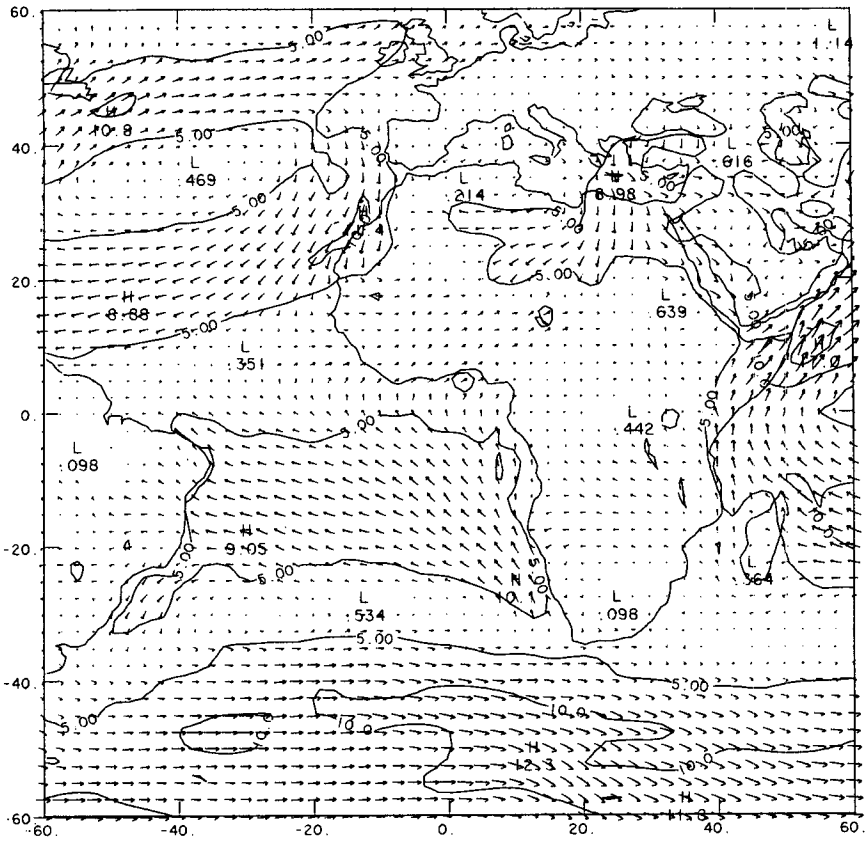


FIG. 4. Mean ECMWF analyzed wind vectors and isotachs at 1000 hPa for July 1985. Contour interval is 5 m $s^{-1}$ and local speed is proportional to vector length.

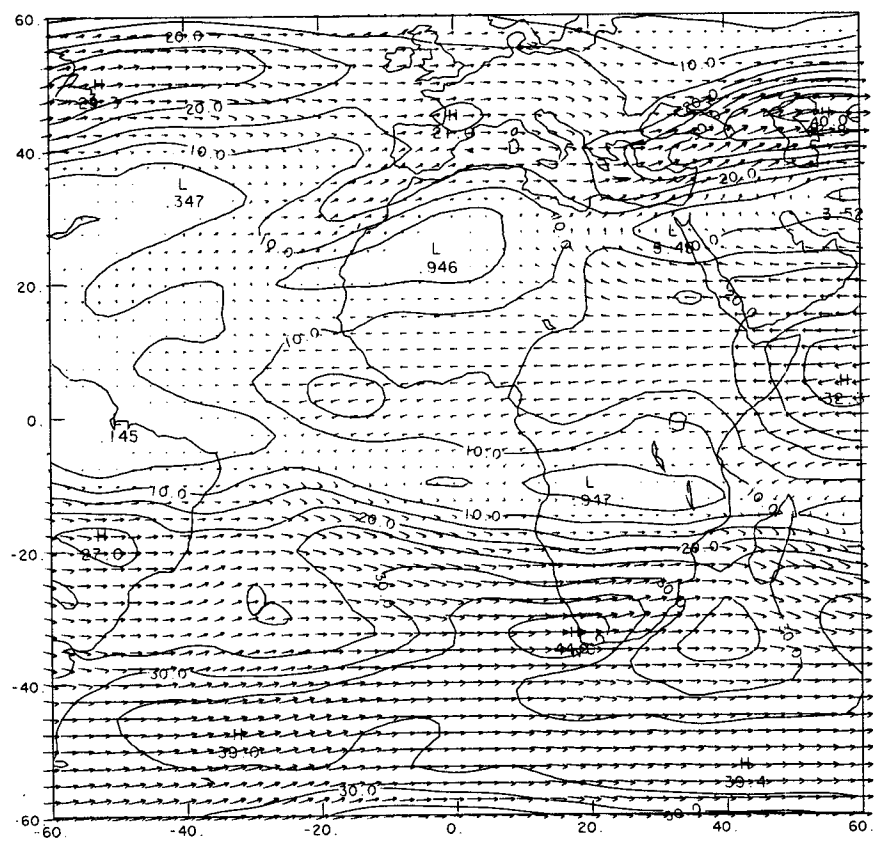


FIG. 5. Same as Fig. 4, but for 200 hPa.

A comparison of these horizontal flows with vertical motions at 500 hPa (Fig. 6) shows that, over the eastern Mediterranean, the diffluence and confluence appearing respectively at 1000 hPa and 200 hPa are associated with a large subsidence. This maximum corresponds to the WV radiance maximum. Over the North Atlantic, a relative maximum of subsidence is located over the region of divergence in the low layers and corresponds to a maximum of WV radiances. In the Southern Hemisphere, subsidence over the western part of the south Atlantic corresponds also with a WV radiance maximum, but the maximum of subsidence over South Africa is shifted southeastward by 2000 km relative to the radiance maximum, due either to a shortcoming of the analyzed field or to an actual tilt of the vertical motion. In the ITCZ, large areas of ascending motion are present, corresponding generally to intense convective activity. Compared with previous results on African convection from satellite data (Desbois et al. 1988), it appears that vertical velocity maxima are well related to convective clouds eastward of Lake Chad. The large ascending motion along the south coast of West Africa, however, is not associated with deep convective clouds, which occur farther north in July.

### c. *Regional study*

To study in more detail the relation between WV radiances and meteorological fields, four test regions have been chosen (Fig. 7). They correspond to major large-scale features of the African climate. Three are associated with subsidence regions in the subtropics, corresponding to high radiances. The fourth spans the ITCZ cloud band and is associated with radiance minima. Figure 8 shows the mean vertical profiles of temperature and relative humidity for the four regions.

Spatial correlations between the monthly averaged WV radiance fields and monthly averaged meteorological fields at six standard levels are computed for each region. The parameters chosen are temperature, relative humidity, vertical velocity, divergence, and geopotential. The spatial correlations obtained are then plotted versus the altitude for each parameter. The level where the correlation is the strongest is the best-fit level of the two fields.

#### 1) SOUTH TROPICAL AREA (AREA 1)

The vertical variation of the WV radiance–temperature correlation (Fig. 9a) indicates that radiances have

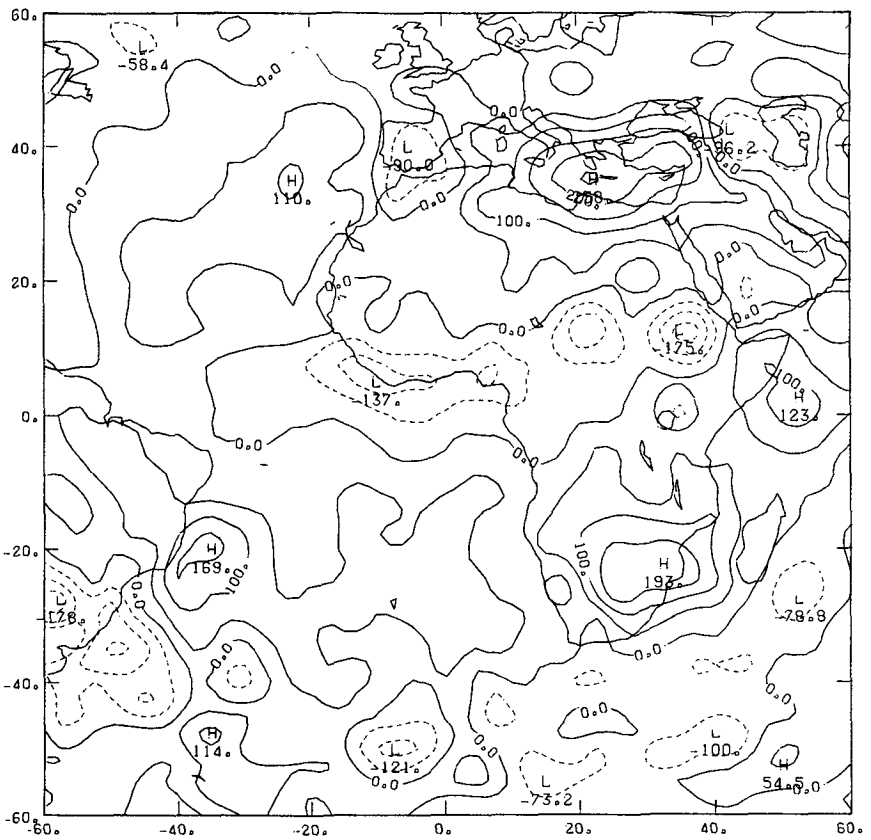


FIG. 6. Mean analyzed vertical velocity at 500 hPa for July 1985. Dashed isolines: negative values or ascending motion. Units: $10^{-3}$ Pa $s^{-1}$. Contour interval is $50 \times 10^{-3}$ Pa $s^{-1}$.

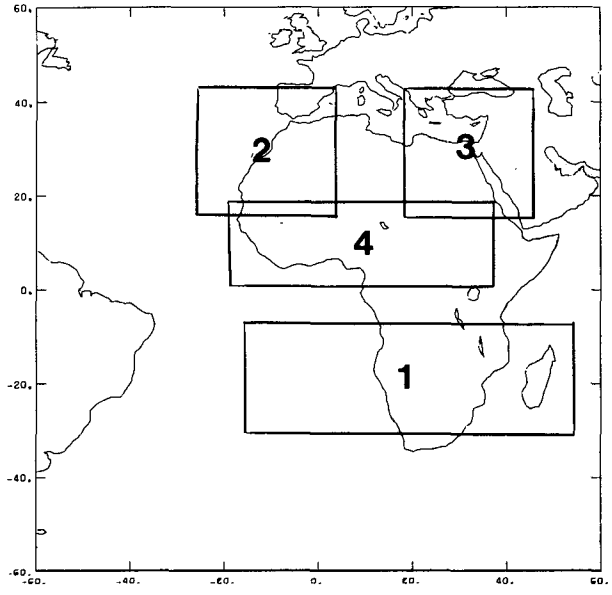


FIG. 7. The four areas chosen for the regional study: 1) south tropical area; 2) western north tropical area; 3) eastern north tropical area; 4) ITCZ.

a spatial structure resembling that of tropospheric temperature for a deep layer extending from 850 hPa to 300 hPa ($r = 0.7$). Indeed, the temperature patterns do not change very much with elevation in this layer: a warm area appears over the continent at 850 hPa, related to the contrast between the cold ocean covered with stratocumulus and the warmer continent (as shown from the infrared imagery by Desbois et al. 1988). This warm area is shifted progressively towards the Atlantic between 700 hPa and 300 hPa. The vertical structure of the correlations is very different for the relative humidity: only the layers 500 hPa to 200 hPa present a high correlation ($r = -0.8$). In this layer, the air is very dry, related to the large-scale subsidence; at 700 hPa and below, the air is humid (Fig. 8b) often containing significant stratiform cloudiness.

The correlation with the vertical velocity (Fig. 9b) is much smaller, maximizing at 700 hPa. The positive correlation is due mainly to the matching of the radiance maximum to a vertical velocity maximum along the Angola coast. Above 700 hPa, the correlation decreases, due to a southeastward shift of the subsidence relative to the radiance maximum.

The radiance–divergence correlation is weak because of noise in the divergence field. Nevertheless, the correlation reverses sign between the top and the bottom of the troposphere because a large WV radiance is associated with divergence at the bottom and convergence at the top of the troposphere.

The radiance–geopotential correlation changes sign between 850 and 700 hPa and maximizes at and above 700 hPa. In this permanent anticyclonic zone, the pressure, temperature, and humidity fields are well correlated and thus also correlated with the WV radiances. Moreover, the analyzed mass field is more reliable than the humidity or vertical velocity field, thus yielding the largest correlations. The change of the correlation sign near the surface shows a shift of the geopotential structure between the surface and the middle troposphere, at least in the ECMWF analysis, since the WV radiances do not represent the lower levels.

### 2) WESTERN NORTH TROPICAL AREA (AREA 2)

Radiance–temperature correlations are best at 700 hPa (Fig. 10a), where the curvature of the isotherms resembles the curvature of the radiance isopleths. As in the south tropical area, a warm core is shifted westward from the surface to upper levels, disappearing at 300 hPa. Surprisingly, the radiance-relative humidity correlation is weak in the middle troposphere ($r = -0.4$ at 500 hPa). At 300 hPa, the correlation becomes very good ($r = -0.85$).

The radiance–vertical velocity correlation is very poor at all levels. In the western part of this area, subsiding motions exist; elsewhere, the vertical velocities described by the model analysis are very weak. The water vapor distribution depends more strongly on horizontal advection in this region. For the same reason, the radiance–divergence correlation is not significant in this region.

Radiance–geopotential correlations are maximum at and above 700 hPa, with a reversal near the surface.

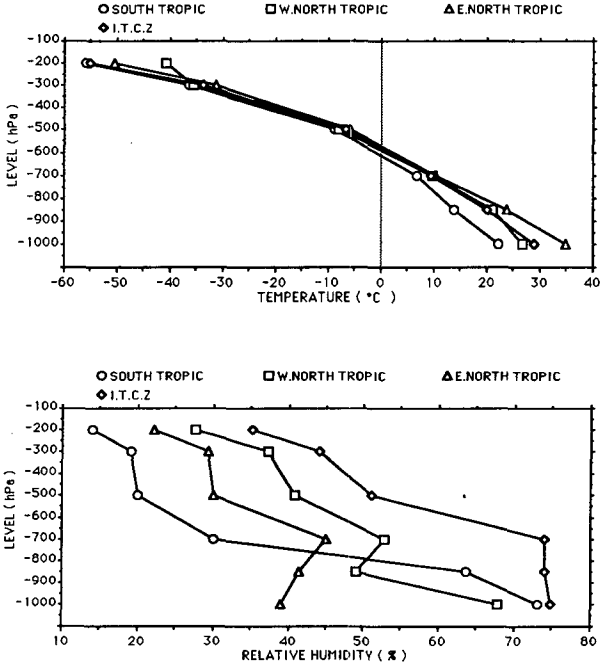


FIG. 8. Vertical profiles of the mean analyzed temperature (top) and the mean analyzed relative humidity (bottom) for the four regions of Fig. 7.

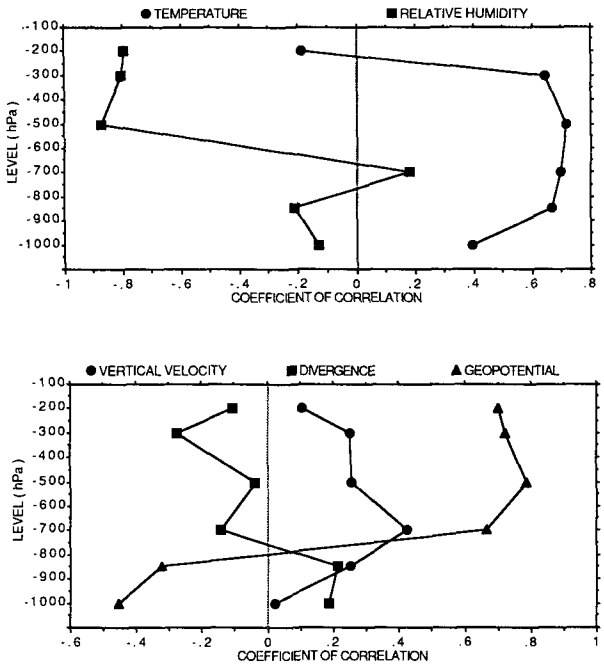


FIG. 9. For the south tropical area, the vertical variation of the spatially averaged correlation between the mean WV radiances and: (top) mean temperature and relative humidity, and (bottom) vertical velocity, divergence, and geopotential.

The vertical structure of these correlations closely resembles that of area 1, due to the meteorological similarities of these areas: area 2 includes the southern part of the Azores high and the western part of the Saharan thermal low. Near the surface, the thermal low dominates the structure of the pressure field, but at higher levels the region is dominated by the large-scale anticyclone. For the same reasons as for region 1, this large-scale structure influences the water vapor distribution, inducing significant correlations with the radiances.

### 3) EASTERN NORTH TROPICAL AREA (AREA 3)

Temperature and WV radiances are correlated strongest at high levels (Fig. 11a), due to the presence of warm air over the eastern Mediterranean Sea at these levels. The temperature fields are much smoother, however, than the WV radiance fields.

The best correlations with relative humidity occur at and below 500 hPa. Indeed, at 850 hPa, a dry-air region is present over the eastern Mediterranean Sea, with higher humidities to the south and west. This structure is very similar to the radiance structure ($r = -0.9$ at 850 and 700 hPa). Above 500 hPa, the minimum of analyzed humidity is shifted eastward relative to the radiance maximum, causing a decrease in the correlation.

The radiance–vertical velocity correlations (Fig. 11b) are larger than in the other regions for all levels above 850 hPa. Indeed, the model analysis shows subsidence, clearly associated with convergence at high levels. Thus, the radiance–divergence correlation is also significant, with a change of sign between the top and the bottom of the troposphere, indicating convergence in altitude and divergence near the surface.

The WV radiances are not well related to the geopotential. A part of this area corresponds to the eastern part of the Saharan low in the lower layers. Anticyclonic conditions prevail above and explain the reversal of sign of the correlations with altitude as in area 2. Because the divergent motions and vertical velocities are larger, however, the structure of the pressure field has less influence on the humidity distribution. The weak correlations with the geopotential have to be compared with the radiance–temperature correlations.

### 4) ITCZ AREA (AREA 4)

In this region where cold cloud tops frequently occur, the mean WV signal results from a combination of radiances emitted from the top of these clouds and atmospheric water vapor when no cloud is present. The general structure of the field, however, is governed mostly by the more or less frequent presence of cold-topped clouds, which modulates the signal more than variations in the water vapor content. Thus, the interpretation of correlations between the radiances and the meteorological fields has to be different. For example, a radiance–relative humidity correlation maximum is found at 700 hPa (Fig. 12a). This level corresponds to the top of the very humid, low layers of this area (Fig.

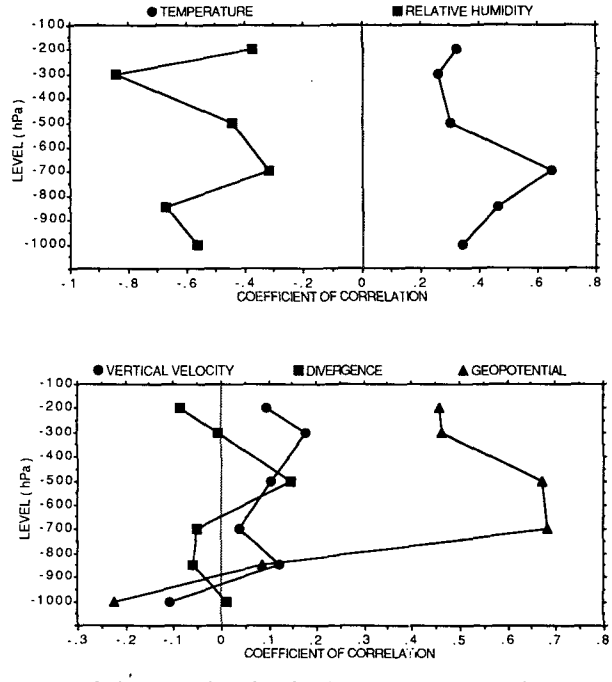


FIG. 10. Same as Fig. 9 but for the western north tropical area.

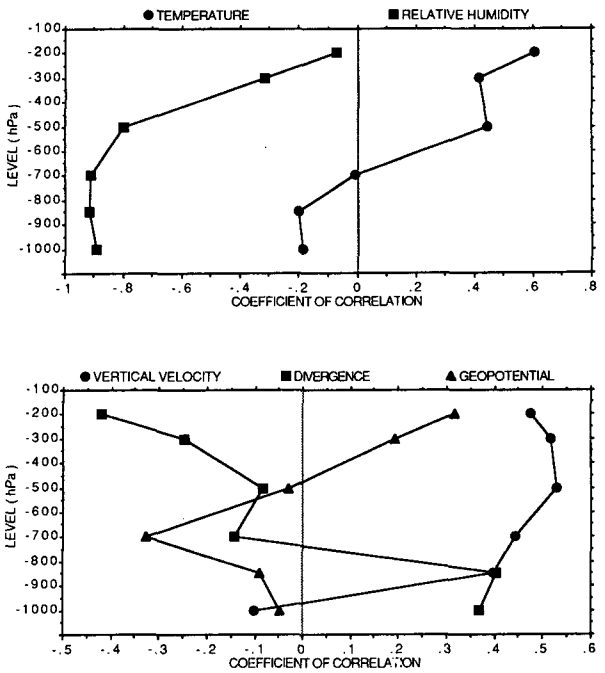


FIG. 11. Same as Fig. 9 but for the eastern north tropical area.

8b), and the structure of the mean humidity field at 700 hPa is similar to the convective cloud distribution as observed by the satellite; the most humid regions at 700 hPa are related to convective activity. This relationship does not hold so well at upper levels. It is unclear whether the weaker correlations aloft result from atmospheric convective processes or as an artifact of ECMWF model parameterizations.

Correlations with the dynamical parameters (Fig. 12b) are poor, in connection with the abnormal ascending motion over the south coast of West Africa, which is not associated with convective clouds (see discussion in section 4b).

## 5. Temporal correlations

The previous statistical results have shown that some information about the large-scale atmospheric structure and circulation can be inferred from the mean monthly radiance fields in the WV channel of METEOSAT. One can question now if the same kind of results can be obtained from individual WV fields. To test this possibility, temporal correlations are computed between time series of METEOSAT WV radiances and time series of the corresponding meteorological parameters. Computations are based on WV radiances at 1130 UTC for a given region for each day of July 1985 and ECMWF analyzed fields at noon in the same region. Two sizes of regions have been chosen: a large size, corresponding to the same regions in Fig. 7, to check the detectability of temporal changes in the large-scale circulation; and a very small size (3 × 3 pixels) to test the relationship with smaller-scale systems.

For the large regions already used to study the monthly spatial correlations, the temporal correlations are poor. The relative humidity is still the best-correlated parameter (Fig. 13), but the coefficient of temporal correlation does not exceed 0.4, whereas the mean field was correlated with the mean radiance field at a level of 0.9. The only other noticeable correlations occur in region 3 (eastern north tropical area) for the vertical velocity (Fig. 14). This is an interesting result, when we consider that the time variations of the parameters averaged over such large regions are very small.

To eliminate the large spatial averaging and to separate the time domain from the space domain, correlations were computed over small regions of 3 × 3 pixels, chosen in the center of the radiance extrema. The temporal correlations obtained were weaker still than those in the large areas, with signs changing more randomly.

These very poor temporal correlations are discouraging, but they do not mean that no information on the temporal variations of the atmospheric parameters can be deduced from the WV images. Some of the poor results may be due to the radiances: the occasional occurrence of cirrus above dry regions, which does not affect the mean fields significantly, can be very damaging for the temporal correlation. The lack of correlation can be attributed also to the inability of the model analysis to reproduce short time-scale fluctuations in the tropics; this conclusion was already reached by

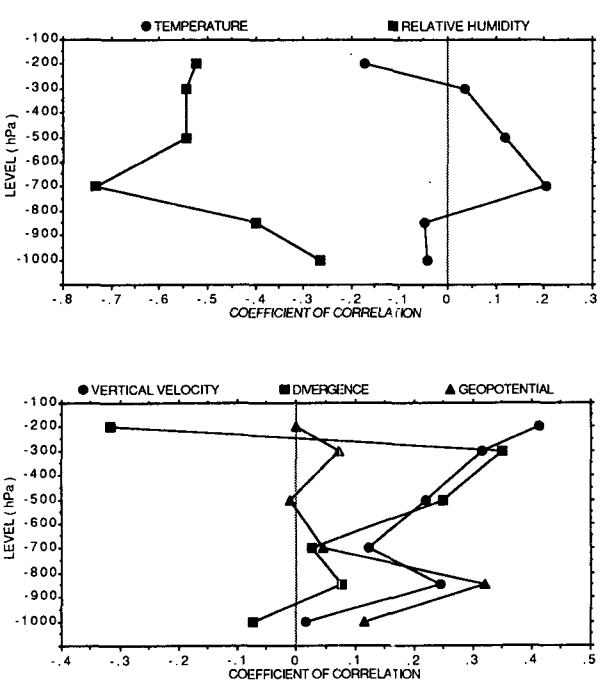


FIG. 12. Same as Fig. 9 but for the ITCZ.

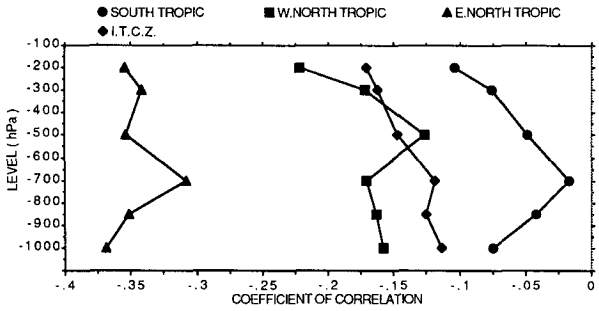


FIG. 13. Vertical variation of the temporal correlation between the WV radiance and the analyzed relative humidity, for the four regions of Fig. 7.

McGuirk et al. (1989) in studying synoptic-scale moisture variations using ECMWF model analyses and satellite data. A major drawback of the analyses is that in the tropical regions under consideration, the observations are very scarce, so that the analysis is only a slight modification of the first guess, which reproduces the mean motions but not necessarily the daily fluctuations in the tropics. In addition, slight spatial shifts are observed between the temporally averaged fields; the effect of these shifts on the correlation becomes more drastic when small regions and short time scales are considered.

However, other studies (Desbois et al. 1988; Reed 1988) have yielded useful comparisons between analyzed fields and satellite radiances on daily scales. These comparisons, though, are based on tracking weather systems, and the precise localization of the tracked phenomena is not crucial. The only analyzed parameters used in these studies were winds. On the other hand, computing correlations here has required a good colocation of several parameters.

## 6. Conclusion

The aim of this study was to demonstrate the usefulness of water vapor channel data for the description of large-scale atmospheric features in the tropics. For this purpose, the ECMWF analyses were taken as the best "in situ truth." However, the results obtained at different time scales suggest that the method chosen here to compare both kinds of fields can be used only for climatic comparisons, e.g., at monthly scales, but not for describing instantaneous fields or time variations. For these smaller scales, time series of direct measurements over particular areas would be more appropriate. Other methods, based on tracking tropospheric structures (cloud-winds, easterly waves), show better agreement between analyses and radiances, probably because they do not need such a precise localization.

The results obtained from correlating the mean monthly WV radiances with different mean monthly meteorological fields obtained from the ECMWF analyses can be summarized as follows:

(i) As expected, relative humidity is the parameter best correlated with the WV radiance, but the layers of best fit are different for the different climate regions—for example, above the 500 hPa level over the subtropical oceanic regions, and below this level in the subtropical region of northeastern Africa.

(ii) There is also a relationship between the WV radiances, hence the water vapor distribution, and the divergent part of the wind, which is noticeable mainly from the presence of high level convergence and midtropospheric subsidence in regions with high WV radiances; the correlations are not very high, due partly to the processes involved in maintaining the water vapor distribution and partly to the noise in the analyzed fields of these parameters.

(iii) This relationship appears to be different for different regions, as horizontal advection also plays a role in the water vapor distribution; the correlation coefficient is the largest (0.52) over the region northeast of Africa where the mean wind vector in the middle troposphere is the smallest (5.7 m $s^{-1}$) and the smallest ($r = 0.10$ to 0.26) over the Azores and southern tropics where the mean wind vector exceeds 7 m $s^{-1}$.

(iv) In these last oceanic regions, a fair correlation of the radiances with the geopotential field is found, indicating again the role of horizontal transports.

(v) In the ITCZ, the comparisons mainly indicate the position of the ITCZ cloud band relative to the analyzed field, as in previous studies using other IR channels. An interesting co-location is found with the relative humidity at 700 hPa, but the vertical velocity and divergence fields appear misplaced by the ECMWF analyses.

The WV radiance images appear useful, at least at the monthly time scale, to locate the position of the main subtropical subsidence areas, allowing a better description of the vertical circulations of the Hadley or Walker type. The presence of a WV channel on meteorological geostationary satellites is of much help for a global view of these circulations and their interseasonal and interannual variations.

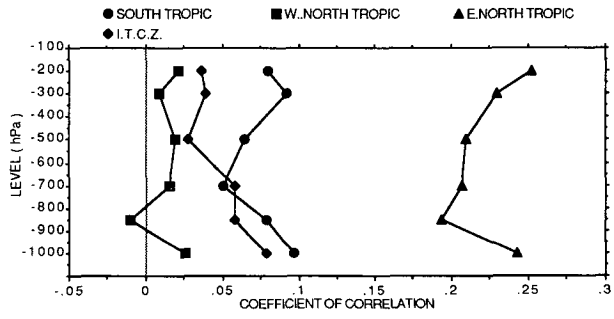


FIG. 14. Same as Fig. 13 but for correlation between the WV radiance and vertical velocity.

A further step in the use of these data would be the quantification of the divergent wind fields and vertical motions over the subtropical anticyclonic areas. One possible way is to take into account both the water vapor radiances from the satellite and the generally reliable horizontal advection from the analysis. Besides its use in diagnostic climate studies, such a method could be used to improve the initialization of the divergent part of the wind in general-circulation models. This approach would be similar to that of Kasahara et al. (1988) who propose a scheme to specify the divergent initial state in an operational model using satellite infrared data to separate ascending and subsiding motions.

Another direction to explore is to use the model to simulate quantities directly observable from the satellite. In the case of the WV radiance fields, this can be done by computing simulated radiances from the analyzed profiles and an appropriate radiative transfer model. Comparisons of the simulated and observed fields would be very fruitful to describe more precisely the deficiencies in the model analysis. A further step would be to introduce the observed values of the radiances in the analysis, using the model physics and dynamics to correct other related quantities such as humidity or the divergent wind. This is not so straightforward, but the recent development of adjoint models allows such a possibility.

*Acknowledgments.* We thank J. Pailleux, G. Sommeria, and J. J. Morcrette for their helpful suggestions and D. Ramond for our collaboration. Thanks also to the reviewers for their suggestions to improve the paper's focus. We are indebted to the European Centre for Medium Range Weather Forecasts for providing us the analyses used here.

This research has been supported by the Centre National d'Etudes Spatiales, the Centre National de la Recherche Scientifique, and the University "Pierre et Marie Curie" of Paris.

## REFERENCES

Ardanuy, P. E., and T. N. Krishnamurti, 1987: Divergent circulations inferred from Nimbus-7 ERB: Application to the 1982–1983 ENSO event. *J. Meteor. Soc. Jpn.*, **65**, 353–370.

Brankovic, C., 1986: Zonal diagnostics of the ECMWF 1984–1985 operational analyses and forecasts. Tech. Rep. No. 57, ECMWF, Reading, U.K.

Desbois, M., L. Picon, T. Kayiranga and G. Seze, 1986: Processing and visualization of image series from geostationnary satellites for climatological purposes. *Proc. of the International Electronic Image Week, Second Image Symp.*, Nice, France, 848 pp. [Available from CESTA/Siggraph France, Paris.]

——, T. Kayiranga, B. Gnamien, S. Guessous and L. Picon, 1988: Characterization of some elements of the sahelian climate and their interannual variations for July 1983, 1984 and 1985 from the analysis of Meteosat ISCCP data. *J. Climate*, **1**, 841–897.

Hollingsworth, A., J. Horn and S. Uppala, 1989: Verification of FGGE assimilations of the Tropical Wind Field: The effect of model and data bias. *Mon. Wea. Rev.*, **117**, 1017–1038.

——, A. C. Lorenc, M. S. Tracton, K. Arpe, G. Cats, S. Uppala and P. Kallberg, 1985: The response of numerical weather prediction systems to FGGE level IIb data. Part I: Analyses. *Quart. J. Roy. Meteor. Soc.*, **111**, 1–66.

Illari, L., 1985: The quality of ECMWF humidity analyses. Workshop on high resolution analysis, 24–26 June 1985, ECMWF, Reading, U.K., 325 pp.

Kasahara, A., R. C. Balgovind and B. B. Katz, 1988: Use of satellite radiometric imagery data in the analysis of divergent wind in the tropics. *Mon. Wea. Rev.*, **116**, 866–883.

Krishnamurti, T. N., and S. Low-Nam, 1986: On the relationship between the outgoing longwave radiation and the divergent circulation. *J. Meteor. Soc. Jpn.*, **64**, 709–718.

Lambert, S. J., 1989: A comparison of divergent winds from the National Meteorological Center and the European Centre for Medium Range Weather Forecasts global analyses for 1980–1986. *Mon. Wea. Rev.*, **117**, 995–1005.

Lorenc, A., I. Rutherford and G. Larsen, 1977: The ECMWF analysis and data assimilation scheme: Analysis of mass and wind fields. Tech. Rep. No. 6, ECMWF, Reading, U.K., 47 pp.

Lorenc, A. C., 1981: A global three-dimensional multivariate statistical interpolation scheme. *Mon. Wea. Rev.*, **109**, 701–721.

Martin, F. L., and V. V. Salomonson, 1970: Statistical characteristics of subtropical jet-stream structures in terms of MRIR observations from Nimbus II. *J. Appl. Meteor.*, **9**, 508–520.

McGuirk, J. P., A. H. Thompson and L. L. Anderson, Jr., 1989: Synoptic scale moisture variation over the tropical Pacific Ocean. *Mon. Wea. Rev.*, **117**, 1076–1091.

Poc, M.-M., M. Roulleau, N. A. Scott and A. Chedin, 1981: Quantitative study of Meteosat Water-Vapor channel data. *J. Appl. Meteor.*, **19**, 868–876.

Ramond, D., H. Corbin, M. Desbois, G. Szejwach and P. Waldteufel, 1981: The dynamics of polar jet-streams as depicted by the Meteosat WV channel radiance field. *Mon. Wea. Rev.*, **109**, 2164–2176.

Raschke, E., and W. R. Bandeen, 1967: A quasi-global analysis of tropospheric water–vapor content from TIROS IV radiation data. *J. Appl. Meteor.*, **6**, 468–481.

Reed, R. J., A. Hollingsworth, W. A. Heckley and F. Delsol, 1988: An evaluation of the performance of the ECMWF operational system in analyzing and forecasting easterly wave disturbances over Africa and the Tropical Atlantic. *Mon. Wea. Rev.*, **116**, 824–865.

Rodgers, E. B., V. V. Salomonson and H. Lee Kyle, 1976: Upper tropospheric dynamics as reflected in Nimbus 4 THIR 6.7 $\mu$m data. *J. Geophys. Res.*, **81**, 5749–5758.

Schiffer, R. A., and W. B. Rossow, 1983: The International Satellite Cloud Climatology Project (ISCCP): The first project of the World Climate Research Programme. *Bull. Amer. Meteor. Soc.*, **64**, 779–784.

Schmetz, J., and O. M. Turpeinen, 1988: Estimation of the upper tropospheric relative humidity field from Meteosat Water Vapor image data. *J. Appl. Meteor.*, **27**, 889–899.

Steranka, J., L. J. Allison and V. V. Salomonson, 1973: Application of Nimbus 4 THIR 6.7 $\mu$m observations to regional and global moisture and wind field analyses. *Quart. J. Roy. Meteor. Soc.*, **114**, 639–664.

Stout, J., J. Steranka and R. A. Petersen, 1984: Vertical displacements of the mid-tropospheric water vapor boundary in the tropics derived from the VISSR Atmospheric Sounder (VAS) 6.7 $\mu$m channel. *Proc. AMS Conf. on Satellite Remote Sensing and Applications*, Clearwater Beach, 300 pp.

Tiedtke, M., W. A. Heckley and J. Slingo, 1988: Tropical forecasting at ECMWF: The influence of physical parameterization of the mean structure of forecasts and analyses. *Quart. J. Roy. Meteor. Soc.*, **114**, 639–664.

Turpeinen, O. M., and J. Schmetz, 1989: Validation of the upper tropospheric relative humidity determined from Meteosat data. *J. Atmos. Oceanic Technol.*, **6**, 359–364.